

# Custom Lab: Measuring Viscosity Using the Couette Flow Model

Alex Cheung, Sean Lin, Aldo Gonzalez Ruiz  
Dept. of Mechanical Engineering, University of California at Berkeley  
(Date: 11/21/2022)

## Abstract

Viscosity is a fluid property that greatly impacts the dynamics of any fluid. Examples include how easily the fluid can flow through a channel, how laminar or turbulent the flow tends to be, and how much mechanical shock absorption capacity the fluid has. While industrial-grade viscometers often measure viscosity by analyzing the flow rate of fluid through a thin tube or by analyzing the torque needed to spin a rotating rod submerged in the fluid, we are attempting to measure viscosity via a testing apparatus that is designed to emulate Couette Flow: the infinite-plate theoretical model used to define viscosity in most introductory fluid mechanics courses. In this lab, we attempt to observe and report on the viscosity-measurement accuracy of a simple rectangular styrofoam block gliding across a meter-long channel filled with fluid.

**Keywords:** Dynamic viscosity, Couette Flow, ultrasonic sensor, image processing, shear stress, velocity gradient, steady-state velocity, fluid depth, surface area, uncertainty propagation.

## 1. Introduction

In this lab, we are measuring the viscosity of two fluids by pulling a boat with a constant force across the fluid surface. We created a channel to house the fluid and used a pulley and mass system to maintain constant shear force. The two directly measured quantities are fluid depth and steady-state velocity. We first use an ultrasonic sensor to measure the depth of the fluid. We then use image processing techniques to determine steady-state velocities which occur when the pulling force and the viscous shear force are acting in equilibrium. The measured data allows us to observe trends in viscosity in conjunction with other factors.

The purpose of this lab is to understand how fluid depth affects the steady-state velocity, as well as compare the experimentally measured steady-state velocity to depth ratio with values from literature. Additionally, the lab aims to understand whether our apparatus is better equipped to accurately measure higher or lower viscosities. Finally, we want to understand the shortcomings of our setup, whether that be the breakdown of theoretical models or unforeseen physical phenomena.

## 2. Theory

### 2.1 Viscosity

Viscosity is a measure of a fluid's resistance to shear stress. Equation (1) is the physical law that describes the relationship between a fluid's viscosity and the shear stress placed on the fluid. Here,  $\tau$  represents the shear stress,  $F$  the shear force,  $\mu$  the dynamic viscosity, and  $dU/dy$  the velocity gradient of the fluid.

$$\tau = \frac{F}{A} = \mu \frac{dU}{dy} \quad (1)$$

For clarification, there are two primary forms of viscosity: kinematic and dynamic viscosity. Kinematic viscosity is the dynamic viscosity normalized by the fluid's density and is thus a measure of velocity rather than force. **For the purpose of this lab, all viscosity values will be dynamic viscosity.** The units for dynamic viscosity are in centipoise or milli-Pascal seconds (1 cP = 1 mPa \* s).

## 2.2 Couette Flow Model

The theoretical model used to derive dynamic viscosity is the Couette Flow model. Couette Flow is characterized by two infinite plates with a uniform layer of fluid between the plates. One of the plates is stationary while the other plate is moving at a constant speed. The fluid in between the plates will move in response to the moving plate. The velocity of this fluid changes with depth, and thus a velocity profile develops within the fluid. Figure 1 depicts a side-view of the velocity profile with Couette Flow on the left [1].

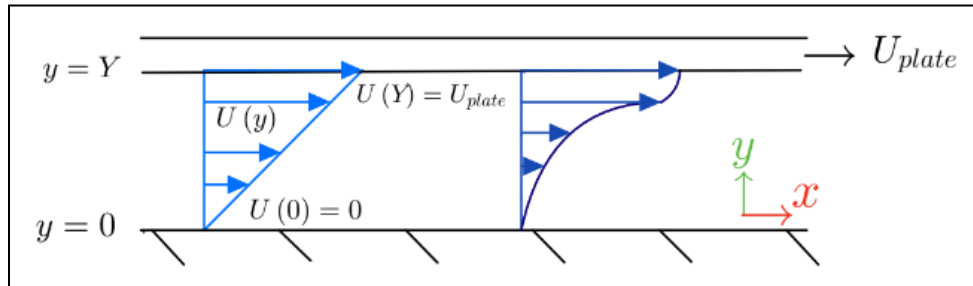


**Figure 1.** Top plate is moving at velocity  $U_{plate}$ . Bottom plate is stationary. Left side is an example of a linear Couette Flow velocity profile. Right side is an example of a non-linear velocity profile.

## 2.3 Assumptions

The first assumption of the Couette model is the no-slip boundary condition. This means that the fluid along any stationary object will also be stationary and the fluid along any object moving at speed  $U$  will also move at speed  $U$  (Figure 1).

The second and most important assumption is the linear velocity gradient assumption. The fluid is expected to have a linear velocity profile similar to the left side in Figure 1. This assumption allows us to assume that the term  $dU/dy$  in Equation (1) can be considered a constant (Equation (2)). With this in mind, Equation (1) can be rearranged into Equation (3), which is the golden formula used in the rest of this lab to calculate measured viscosities.

$$\frac{dU}{dy} = \frac{U_{plate}}{Y} = \text{constant} \quad (2) \quad \mu = \frac{F}{A} \frac{Y}{U_{plate}} \quad (3)$$

## 3. Methods

The apparatus we used to replicate Couette Flow was a meter-long channel filled with fluid. A small, lightweight boat rests on top of the fluid, which is pulled in a horizontal direction by a

constant force provided from the mass on the end of a string. The depth of the fluid was measured by a differential ultrasonic sensor reading, and the velocity was measured using image processing. **The fluids used were Dawn dish soap (theoretical viscosity 396 cP) and Karo corn syrup (theoretical viscosity 2000 cP) [6 & 7].**

### 3.1 Construction of Apparatus

The channel was designed to be long enough to allow the boat enough room to accelerate to a steady velocity. The channel was also designed to have a level bottom face in order to ensure uniform depth. The channel was designed for modularity and consisted of 5 assembled channel segments. Lastly, the channel was designed to be leakproof and wide enough to prevent the boat scraping the sides of the channel. The channel was made using acrylic and bonded together using acrylic cement. It was made leakproof using plumber's sealant and clear tape. At the end of the channel was a 3-D printed pulley which was attached using another 3-D printed structure (Appendix A3). The cross sectional geometry of the channel is depicted in Appendix A4 and A6.

The boat was a simple styrofoam block (nominally 2.0 cm x 8.5 cm x 9.5 cm), chosen for being lightweight thus not sinking significantly. A layer of packaging tape was applied to the surface of the boat that would come in contact with the fluid to prevent any corrosion and to make the critical contact surface more smooth. Two brass loops were attached to the front of the boat as attachment points for the string connected to a mass. Lastly, on top of the boat we attached a wooden stick with a white circle which we used for image tracking.

As a reference for image processing, we used a black backdrop with 9 red circular cutouts evenly spaced 10 cm apart.

### 3.2 Testing Procedure

Before filling the channel with fluid, we measured the empty depth of the channel with an ultrasonic bridge (Figure 2). We took 5 measurements along the channel and averaged them to get the depth of the empty channel. We then set up the black backdrop with the red circles.

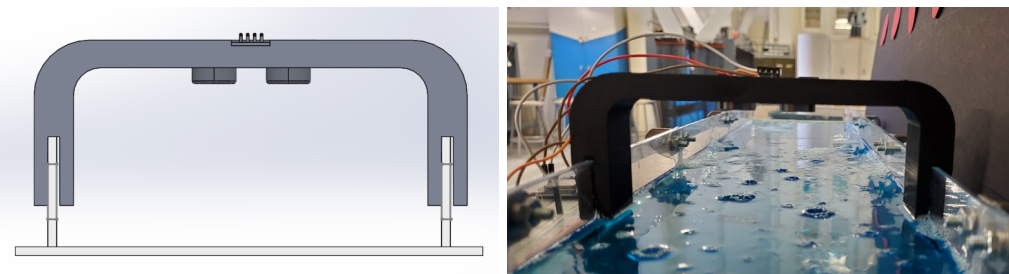


**Figure 2.** Schematic and picture of ultrasonic bridge used to measure fluid depths.

After having everything ready we poured the fluid inside the channel and allowed it to settle. We used the ultrasonic bridge to measure the depth in 5 different locations along the channel once more. We then averaged the values and subtracted them from the initial empty channel value to obtain a depth measurement. A mass was then attached to the other end of the string and placed on the pulley. The boat was released at the far end of the channel from rest, allowing the weight of the mass to pull it at a constant speed, and a side-view video was recorded (Refer to Appendix A1). We recorded every test using an iPhone 11, which has a frame rate of 30fps. The

videos were then cropped and shortened to make edge detection easier. After repeating 4 trials at each depth, more fluid was added and allowed to settle. The aforementioned depth measurement and testing process was repeated a total of 3 depths per fluid. We chose to use Dawn dish soap and Karo corn syrup because they are easily accessible in bulk quantities and also cover a wide range of theoretical viscosities.

### 3.3 Image Processing

For image processing, we ran an edge detection algorithm and determined the number of pixels between the centers of each red dot (Figure 3). We averaged this value and divided it by 10 to obtain a pixels-per-cm scaling value for every video. We then tracked the white circle and plotted its x-pixel coordinate over time. The linear region of the resulting plot was manually isolated and fit to a linear model. The slope of the linear fit was scaled by the pixel-to-cm conversion factor and taken as the measured velocity. The 95% confidence interval of this slope was also scaled and taken as the uncertainty of the measured velocity (Appendix B2). Lastly, a simple script was used to calculate viscosities based on the measured input variables (Appendix B1).

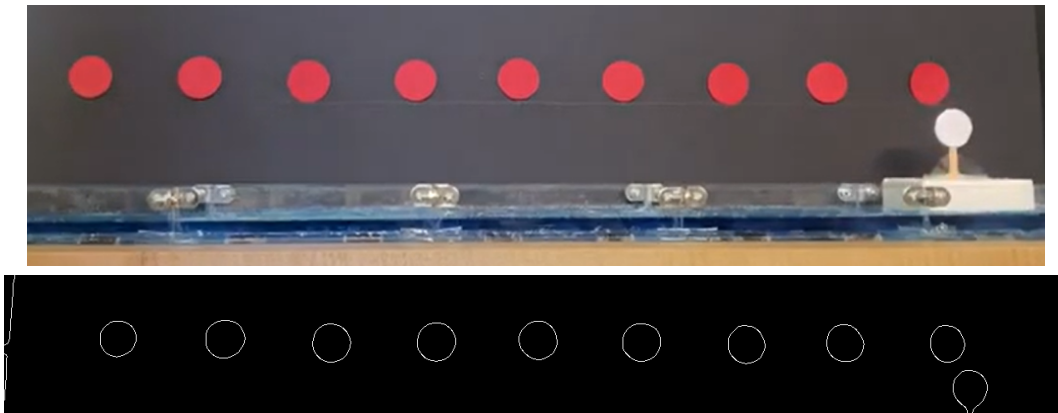


**Figure 3.** An example of a raw frame from the video along with the edge-detected frame

## 4. Results

### 4.1 Raw Results

**Note:** All 12 dish soap tests used a 12.7 gram weight. All corn syrup tests used a 51 gram weight. The area of the boat stayed constant in both liquids at 81.230 cm<sup>2</sup>.

**Table 1.** Dish Soap Test: Depth Measurements (cm)

Segment 1	Segment 2	Segment 3	Segment 4	Segment 5	Average	Empty Channel	Depth of Fluid
4.93	4.93	4.93	5.05	5.05	4.978	5.64	0.662 ± 0.1
4.59	4.57	4.58	4.64	4.69	4.614		1.026 ± 0.1
4.16	4.11	4.16	4.23	4.28	4.188		1.452 ± 0.1

The table above shows the average distance from the fluid to the ultrasonic sensor. Depth of the fluid was calculated by subtracting average values from the empty channel measurement. **All uncertainties are  $\pm 0.15$  cm (ultrasonic sensor datasheet) unless otherwise specified [8].**

**Table 2.** Dish Soap Trials: Results

Trial	Depth (cm)	Velocity (cm/s)	Avg. Velocity (cm/s)	Viscosity (cP)	Avg. Viscosity (cP)
1	$0.6620 \pm 0.1500$	$5.5116 \pm 0.0016$	$5.6424 \pm 0.0034$	$1840.3 \pm 417.0$	$1798.1 \pm 203.8$
2		$5.7459 \pm 0.0041$		$1765.3 \pm 400.1$	
3		$5.6853 \pm 0.0086$		$1784.1 \pm 404.3$	
4		$5.6267 \pm 0.0094$		$1802.7 \pm 408.5$	
1	$1.026 \pm 0.1500$	$6.4115 \pm 0.0050$	$6.3915 \pm 0.0016$	$2451.9 \pm 358.6$	$2459.9 \pm 180.1$
2		$6.4233 \pm 0.0029$		$2447.4 \pm 357.9$	
3		$6.4600 \pm 0.0020$		$2433.5 \pm 355.9$	
4		$6.2712 \pm 0.0016$		$2506.8 \pm 366.6$	
1	$1.452 \pm 0.1500$	$6.7115 \pm 0.0034$	$6.4585 \pm 0.0023$	$3314.8 \pm 342.7$	$3446.9 \pm 178.4$
2		$6.4887 \pm 0.0044$		$3428.7 \pm 354.5$	
3		$6.3518 \pm 0.0067$		$3502.6 \pm 362.1$	
4		$6.2819 \pm 0.0031$		$3541.5 \pm 366.1$	

The table above shows all measured inputs for calculating viscosity as well as the calculated viscosity.

**Table 3.** Corn Syrup Test: Depth Measurements (cm)

Segment 1	Segment 2	Segment 3	Segment 4	Segment 5	Average	Empty Channel	Depth of Liquid
4.81	4.76	4.76	4.76	4.81	4.78	5.64	$0.86 \pm 0.1$
4.57	4.57	4.57	4.57	4.64	4.584		$1.056 \pm 0.1$
4.34	4.34	4.34	4.34	4.4	4.352		$1.288 \pm 0.1$

**All uncertainties are  $\pm 0.15$  cm (ultrasonic sensor datasheet) unless otherwise specified [8].**

**Table 4.** Corn Syrup Trials: Results

Trial	Depth (cm)	Velocity (cm/s)	Avg. Velocity (cm/s)	Viscosity (cP)	Avg. Viscosity (cP)
1	$0.86 \pm 0.1500$	$5.8877 \pm 0.0125$	$6.3439 \pm 0.0041$	$8987.4 \pm 1567.7$	$8356.625 \pm 727.5$
2		$6.4246 \pm 0.0072$		$8236.3 \pm 1436.6$	
3		$6.5265 \pm 0.0057$		$8107.7 \pm 1414.2$	

4		$6.5367 \pm 0.0058$		$8095.1 \pm 1412.0$	
1	$1.056 \pm 0.1500$	$7.0949 \pm 0.0027$	$7.1562 \pm 0.0041$	$9158 \pm 1300.9$	$9079.825 \pm 644.9$
2		$7.1678 \pm 0.0040$		$9064.8 \pm 1287.7$	
3		$7.2166 \pm 0.0082$		$9003.5 \pm 1279.0$	
4		$7.1456 \pm 0.0132$		$9093 \pm 1291.7$	
1	$1.288 \pm 0.1500$	$7.7082 \pm 0.0029$	$7.6422 \pm 0.0062$	$10281.2 \pm 1197.4$	$10370.7 \pm 610.15$
2		$7.6574 \pm 0.0094$		$10349.4 \pm 1205.4$	
3		$7.5609 \pm 0.0218$		$10481.5 \pm 1220.8$	
4		$7.5812 \pm 0.0123$		$10453.4 \pm 1217.5$	

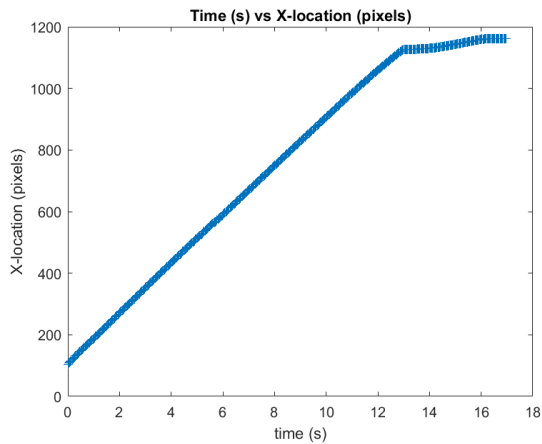


**Figure 4.** Position v. time plot (raw)

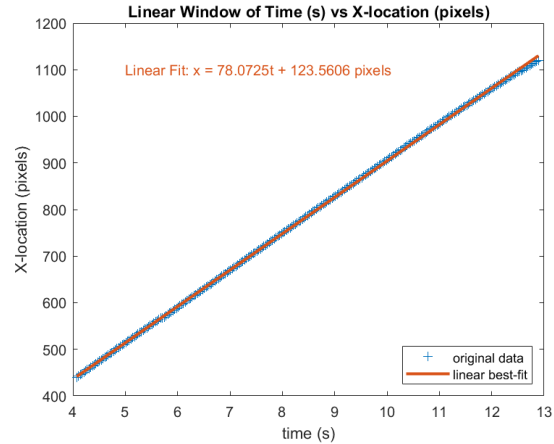


**Figure 5.** Position v. time plot w/ best fit line (cropped)

Figure 4, shows a random soap test that was analyzed through the image processing script. We made sure to capture most of the data points. We then, based on inspection, manually cropped the linear part of the graph to extract the velocity (slope) by linear curve fitting which is shown on Figure 5.

## 4.2 Measurement Uncertainty

For the overall uncertainty of the viscosity we had to calculate the intermediate uncertainties of the ultrasonic sensor, scale, calipers, and image processing. These quantities were used in Equation (4).

$$u_{\mu} = \sqrt{u_F^2 \frac{\partial \mu}{\partial F}^2 + u_y^2 \frac{\partial \mu}{\partial y}^2 + u_A^2 \frac{\partial \mu}{\partial A}^2 + u_U^2 \frac{\partial \mu}{\partial U}^2} \quad (4)$$

The uncertainty of the force from the mass is represented by  $u_F$ . Similarly,  $u_y$ ,  $u_A$ ,  $u_U$  are the uncertainties of the depth, area, and velocity respectively. Meanwhile the partial derivatives are taken through differentiating Equation (3), with respect to each variable.

$$\frac{\partial \mu}{\partial F} = \frac{y}{AU} \quad (5)$$

$$\frac{\partial \mu}{\partial y} = \frac{F}{AU} \quad (6)$$

$$\frac{\partial \mu}{\partial A} = \frac{Fy}{U} \quad (7)$$

$$\frac{\partial \mu}{\partial U} = \frac{Fy}{A} \quad (8)$$

Equations (5) through (8), show the partial derivative of Equation (3) with respect to each variable. Note that we treated  $dy/dU$  as  $y/U$  for the purpose of facilitating these derivatives and to quantify our uncertainty.

$$u_x = \frac{\sqrt{u_{x1}^2 + u_{x2}^2 + u_{x3}^2 \dots}}{N} \quad (9)$$

$$u_F = u_w g \quad (10)$$

$$u_A = \sqrt{u_c^2 w^2 + u_c^2 l^2} \quad (11)$$

When calculating the uncertainty of an average of multiple independent values, we can generalize the formula to Equation (9) [4]. Equation (9) was used to calculate the uncertainty of the velocity ( $u_u$ ), we took the 95% confidence interval of each velocity using the MATLAB fit function and divided the interval by 2 to get the uncertainty of each trial. We then found the average uncertainty with respect to each depth using Equation (9), which yields 3 uncertainty values per fluid (one for each depth).

We took 5 different depth measurement readings with the ultrasonic sensor per depth, and used Equation (9) as well. We calculated the uncertainty of the samples, by taking the datasheet resolution value and dividing it by 2. This was also done to find the uncertainty in the caliper ( $u_c$ ), and in the scale ( $u_w$ ). After accurately finding these uncertainties, we were able to calculate the uncertainty of the measurement (Appendix B4).

For the uncertainty of the force, we took the uncertainty of the scale ( $u_w$ ), and multiplied it by the gravitational constant ( $g$ ). Equation (11) calculates the uncertainty of the area through caliper resolution ( $u_c$ ), where  $w$  is the width and  $l$  is the length. Lastly, we plugged all the calculated values from Equations (5)-(11) into Equation (4) to get the uncertainty of the viscosity below:

**Table 6.** Values of the viscosity uncertainties at tested depths.

	Depth 1	Depth 2	Depth 3
Dish Soap	<b>± 203.8 cP</b>	<b>± 180.1 cP</b>	<b>± 178.4 cP</b>
Corn Syrup	<b>± 727.5 cP</b>	<b>± 644.9 cP</b>	<b>± 610.15 cP</b>

**Note:** The liquids did not have the same depth, each depth is respective to their liquid.

## 5. Discussion

### 5.1 Observed Trends

Based on the data obtained, our results deviate from the ideal model as we increased the depth of the fluid. Figure 6 below shows the rate at which dish soap and corn syrup measured viscosities deviate from the theoretical values used in this experiment. See Appendix B3.

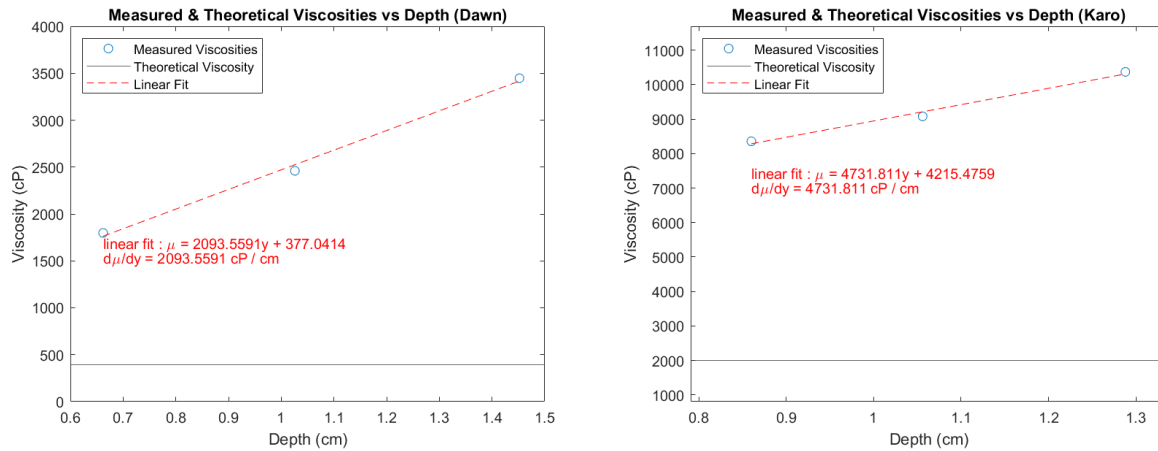


**Figure 6.** Viscosity v. depth for dish soap(left) & corn syrup(right) with theoretical & experimental trends

The image on the left gives us the line of best fit for the change in viscosity of dish soap with respect to depth, while the one on the right shows the same for corn syrup. We can see that  $d\mu/dy$  of dish soap is much smaller than  $d\mu/dy$  of the corn syrup. This demonstrates a very clear trend. As the theoretical viscosity of the liquid increases, the Couette Flow model decomposes at a faster rate with respect to depth. Thus testing less viscous fluid like water will give a more accurate reading based on our current set up, and vice-versa. Furthermore, we see a similar trend across each fluid, where the measured values for the first few tests are about 4 to 5 times greater than the theoretical viscosity (Table 7). Although dish soap's absolute rate of viscosity deviation ( $d\mu/dy$ ) is lower than corn syrup's (Figure 6), the relative rate of deviation compared to each fluid's theoretical viscosity is still higher in dish soap (Table 7).

**Table 7.** Ratio of observed viscosity to theoretical viscosity

	Depth 1	Depth 2	Depth 3
Dish Soap	4.54	6.21	8.7
Corn Syrup	4.17	4.53	5.18

**Note:** The liquids did not have the same depth, each depth is respective to their liquid.

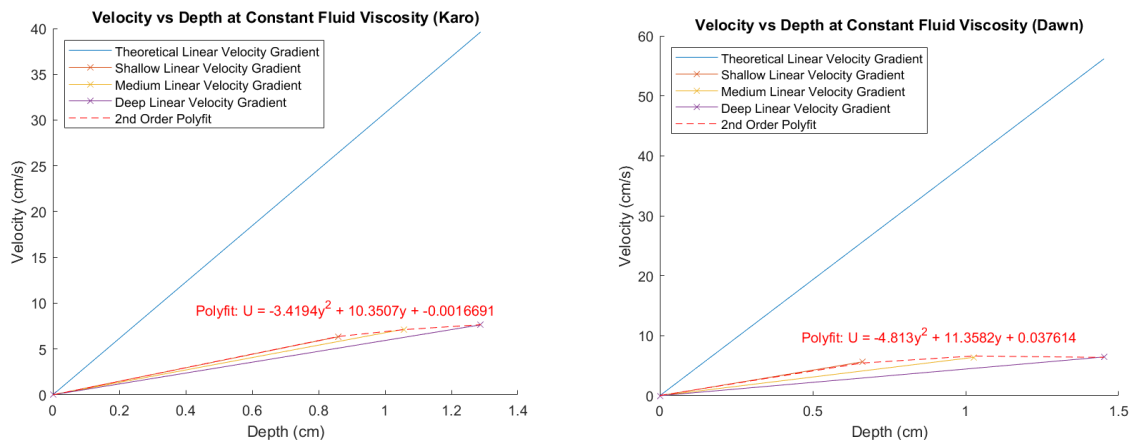


**Figure 7.** Velocity v. depth for dish soap(left) & corn syrup(right) with theoretical & experimental trends



It is possible that the scaling error of our viscosities is either due to the fact that the magnitude of the measured linear velocity profile  $dU/dy$  is different from the magnitude of the theoretical linear velocity profile or due to the fact that the the velocity profile is not linear at all. To answer this question, we plotted measured velocity as a function of measured depth in Figure 7.

These plots can effectively be interpreted as a velocity profile  $dU/dy$ . The blue line represents the linear theoretical velocity gradient, which can be calculated from the theoretical values of viscosity for dish soap and corn syrup. The three points marked with “x” represent the average measured velocity and depth. The line between the origin and each “x” indicates a hypothetical linear velocity profile at each depth. The origin is taken as an implied datapoint.

We can see that with increasing depth, the hypothetical linear velocity profiles from our data deviates further from the theoretical linear velocity profile since successive lines are angled farther and farther away. If the true velocity profile is linear, the three points marked with x should also be collinear. In this case, the differences in the slope of the theoretical and true profiles would represent the difference in the magnitude of the linear gradient. However, since these points are not collinear, the data strongly suggests that the true velocity profile under the boat follows a nonlinear profile. To visualize this, we fitted a 2nd-degree polynomial to the three x's along with the origin as a suggestion for a more accurate mathematical model of the true velocity profile.

## 5.2 Errors Due to Testing Apparatus Shortcomings

### 5.2.1 Boat Sink and True Depth

To calculate the depth with which the boat would sink, we can use Archimedes' Principle (Equation (12)).

$$F_B = \rho V g \Rightarrow m_b g = \rho_f l w y_{sink} g \quad (12)$$

Thus, using the mass(7.0 g), the dimensions of the boat, and the density of the fluid, we can calculate the depth with which the boat will sink using Equation (13). We can then calculate the true depth using Equation (14). Our assumption is that the mass of the boat is uniformly distributed and therefore the boat sinks uniformly.

$$y_{sink} = \frac{m_b}{\rho_f l w} \quad (13) \quad y_{true} = y_{measured} - y_{sink} \quad (14)$$

The true depth is less than the measured depth, which implies that the true viscosity should be less than the measured viscosity per Equation (3). This is consistent with our data which systematically overestimates viscosity and hence this is a potential source of error. However, the depth with which the boat sinks is difficult to accurately measure in practice and was not considered due to an insignificant estimated effect.

### 5.2.2 Drag Force

Since a portion of the boat will dip below the fluid's surface, hydrodynamic drag becomes a factor. Drag force is given by Equation (15).

$$F_D = \frac{1}{2}\rho_f U^2 C_D A \quad (15)$$

Drag force is proportional to the area of the body in cross flow, the velocity of the body, and the density of the fluid. A portion of the force provided by the hanging mass will work to overcome drag, which makes the  $F$  term in Equation (3) smaller than measured. Thus, true viscosity should be less than measured viscosity, which is once again consistent with our data [5].

One significant but unquantifiable factor contributing to drag is the formation of a bow wave at the front of the boat. This wave is caused by a high-pressure region at the front of the boat which forces fluid upward, causing the front of the boat to be submerged deeper than originally anticipated using Archimedes' Principle, causing more drag force to act on the boat.

### 5.2.3 Settling Time

The settling time was a possible error encountered specifically with repeated trials at each depth. As mentioned in the previous section, as the boat increases in velocity, a bow wave builds up in front of the boat and fluid is displaced towards the other end. Since they are high viscosity fluids, it takes a long time for the fluid's surface to return to equilibrium. This was most apparent when testing corn syrup at larger depths. After every trial, we manually displaced the fluid back to the shallower side of the channel, and then let the fluid naturally settle. However, taking these precautionary measures did not necessarily result in a perfectly level fluid. This varying depth along the channel can unpredictably impact the velocity of the boat.

### 5.2.4 Ultrasonic Sensor Error Propagation

After inspection of the uncertainty propagation, we concluded that most of the uncertainty was due to the ultrasonic sensor we used for depth measurement. This is because the resolution of the sensor is 3 mm according to the datasheet [8], which is about half of the shallowest depth measurement in the soap test. Furthermore, this notion is supported by the fact that our viscosity uncertainty decreases as we increase the depth of the liquid, shrinking the ratio between the resolution and measured depth.

### 5.2.5 Non-level Table

When conducting the experiment, the table was not perfectly level. Due to the tilt of the table the fluid depth was not constant across the channel, thus impacting our results. However, averaging the measurements for each channel segment helped to minimize the error, thus we consider this error negligible. Additionally, the non-constant fluid depth may not obey the rules of the theoretical model of Equation (3).

### 5.2.6 Pulley Friction & Inertia

Another possible source of error was friction between the pillow block and the spinning pulley axle as well as the rotational inertia of the wheel. The inclusion of these factors in this pulley system can slow down the velocity of the boat. The weight on the string is used to overcome these forces as well as pull the boat. Once again this demonstrates that the forces used in our calculations were overestimates, making the measured viscosity overestimates, which is consistent with our data. However, given that the coefficient of friction between the brass axle and the PLA housing is very low and the wheel is extremely light, we believe we can consider these energy losses to be negligible.

### 5.2.7 Unequally Spaced Red Markers

Due to human error, we were unable to perfectly space the red markers 10 cm apart on the black background. Because of this, our pixel-to-cm conversion factor has inherent but unquantifiable uncertainty. This creates an unpredictable effect on the measured velocities.

## 5.3 Errors Due to Theoretical Model Inaccuracy

From the trends in the data in Figure 7, it is clear that a linear velocity profile is not a realistically safe assumption.

### 5.3.1 Continuity and Control-Volume Analysis

First, the linear velocity profile can only be safely assumed for the Couette model with infinitely large plates. This can be explained via the law of fluid continuity and demonstrated via control-volume analysis. Under an infinite plate, fluid moving along with the plate is only allowed to move like so because the fluid directly in front of it is moving out of the way at the same velocity. Any control volume drawn underneath the infinite plate obeys continuity and hence a linear flow profile is possible (Figure 8). However, the boat used in this experimental setup was finite in size which causes anomalies at the forward and aft end of the boat. On each of the ends, the fluid immediately before or after the boat must also have a velocity profile that roughly follows the boat to satisfy continuity at CV 1 and 2. However, these profiles are turbulent, non uniform across space, and unpredictable (green arrows) which clearly violate the assumptions in the theoretical model [9].

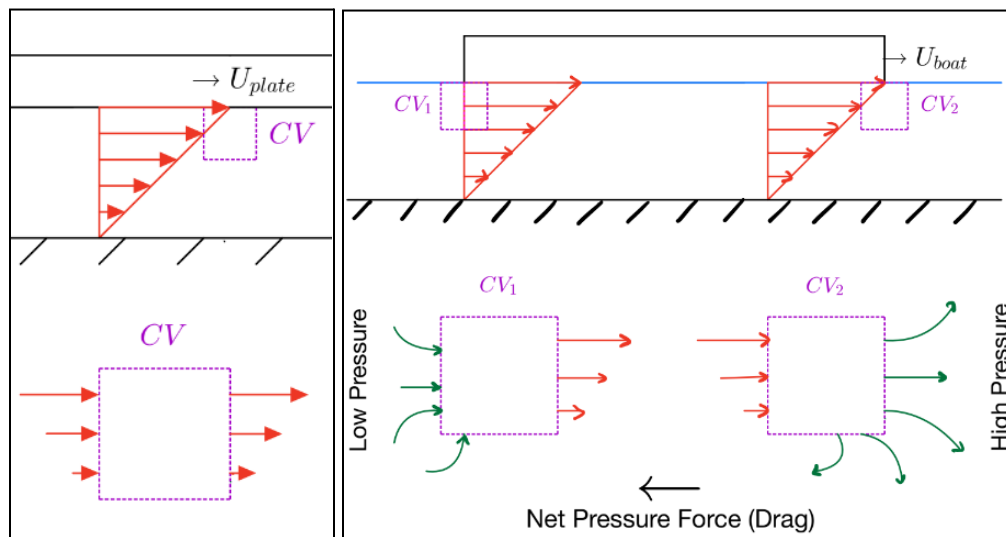


**Figure 8.** Infinite plate mode(left) and finite plate model(right)

### 5.3.2 Pressure Gradient & Couette-Poiseuille Flow

As well, by nature of any projectile moving through a fluid, areas of high pressure are generated at the forward end of the projectile and areas of low pressure at the aft end. This means that there is a net pressure difference between the forward and aft end of the boat as it is being dragged through the fluid. This results in an interesting phenomenon where a fluid wants to move forward through viscous effects (Couette component), yet simultaneously wants to move backwards due to a pressure gradient (Poiseuille component). The resulting profile is fittingly named Couette-Poiseuille Flow and may be a more accurate representation of the true pressure gradient (Figure 9).

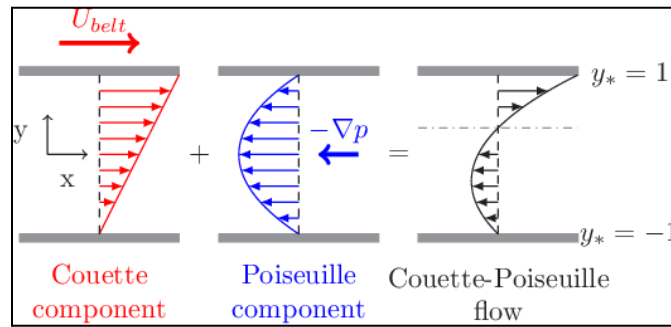


**Figure 9.** Couette-Poiseuille [3]

### 5.3.3 No-Slip Wall Effects

Finally, limitations of the width of the channel also play a role in deviating from the linear velocity profile. This is because the walls of the channel act as additional points of no-slip boundary conditions and effectively pull back on the fluid from the sides. Up until now, the velocity profile has been considered to be independent of  $z$ -position (defined as into the paper plane). However, the walls of the channel create a true velocity profile that becomes weaker towards the sides of the channel (Figure 10). As seen in the figure, the velocity of the fluid must converge to 0 at both the bottom and sides of the channel rather than just the bottom of the channel.

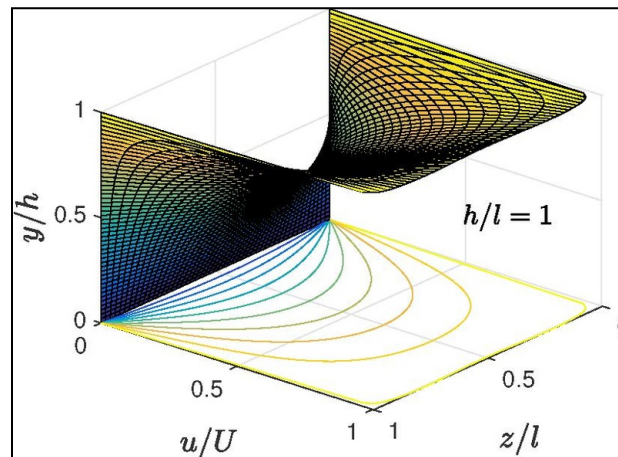


**Figure 10.** Wall-limit [2]

## 6. Conclusion

The experiment conducted in this report measured the dynamic viscosity of the two fluids while following a theoretical model. This was done by measuring the velocity of an object sliding on top of the fluid, and measuring needed quantities such as depth, force, and area. From the data we observed multiple trends. With the current setup, we concluded that a fluid with a higher viscosity will deviate from the model at a faster rate than a lower viscosity fluid. Furthermore, it was seen that increasing the depth in each fluid also leads to more deviation from the model. Lastly, it was concluded that in our lab set up yielded a measured viscosity about 5 times greater than the ideal viscosity, which we can assume will hold true across other Newtonian fluids.

## Contributions

Sean Lin was fully responsible for building the channel apparatus and partially responsible for testing it. He was partially responsible for designing the ultrasonic bridge and fully responsible for manufacturing it. He was also fully responsible for deriving the velocity from the edge-detected image by finding the pixel-to-centimeter conversion factor and fitting a linear curve to the displacement profile. He was also fully responsible for the script used to calculate viscosity as well as the trend analysis scripts and plots. He was fully responsible for understanding and reporting on the theoretical Couette flow model used as well as identifying and reporting the shortcomings of this theoretical model.

Aldo Gonzalez Ruiz was responsible for coding the ultrasonic sensor, which enabled us to get depth readings. In addition, he coded the edge detection code and found optimal settings to ensure the detection of the circles. He also cropped and cut the videos(data) to ensure compatibility with the edge detection. Furthermore, he was partially responsible for designing the ultrasonic bridge and testing. In the lab report, he explained the trends observed in the experiment, and tackled the methods and results.

Alex Cheung was fully responsible for building the backdrop for image processing and partially responsible for testing it. He was partially responsible for setting up the ultrasonic sensor, having set up most of the hardware. In the lab report, he was responsible for describing errors associated with the inherent setup of the experiment as well as the introduction and conclusion portions of the write up.

All three group members contributed equally to the physical testing and lab write up.

## References

- [1] "Couette flow," Couette Flow - an overview | ScienceDirect Topics. [Online]. Available: <https://www.sciencedirect.com/topics/engineering/couette-flow> . [Accessed: 21-Nov-2022].
- [2] "File:Couetter.pdf - Wikipedia." [Online]. Available: <https://en.wikipedia.org/wiki/File:Couetter.pdf> . [Accessed: 21-Nov-2022].
- [3] L. Klotz, G. Lemoult, I. Frontczak, L. Tuckerman, and J. Wesfreid, "[PDF] Couette-Poiseuille flow experiment with zero mean advection velocity: Subcritical transition to turbulence: Semantic scholar," undefined, 01-Jan-1970. [Online]. Available: <https://www.semanticscholar.org/paper/Couette-Poiseuille-flow-experiment-with-zero-mean-Klotz-Lemoult/4e6d00a1d2c50de040c48036d124b2248ab1fc42> . [Accessed: 21-Nov-2022].
- [4] "Uncertainty in the average of two measurements (with their respective uncertainty)," Physics Stack Exchange, 01-May-1965. [Online]. Available: <https://physics.stackexchange.com/questions/392016/uncertainty-in-the-average-of-two-measurements-with-their-respective-uncertainty> . [Accessed: 21-Nov-2022].
- [5] "Physics," Drag Forces | Physics. [Online]. Available: <https://courses.lumenlearning.com/suny-physics/chapter/5-2-drag-forces/> . [Accessed: 21-Nov-2022].
- [6] W. L. Elban, "Viscosity of household fluids - materials education (matedu)." [Online]. Available: [https://materialseducation.org/educators/matedu-modules/docs/viscosity\\_of\\_household\\_fluids.pdf](https://materialseducation.org/educators/matedu-modules/docs/viscosity_of_household_fluids.pdf) . [Accessed: 21-Nov-2022].
- [7] "Viscosity chart," Ellsworth Adhesives. [Online]. Available: <https://www.ellsworth.com/resources/viscosity-chart/> . [Accessed: 21-Nov-2022].

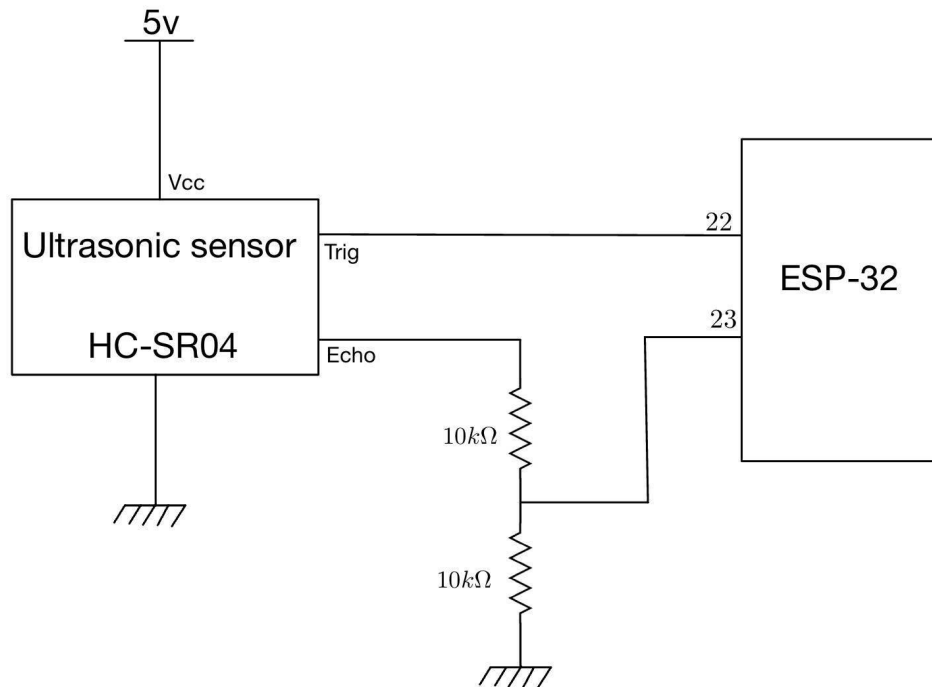
[8] "Ultrasonic ranging module HC - SR04 - SparkFun Electronics." [Online]. Available: <https://cdn.sparkfun.com/datasheets/Sensors/Proximity/HCSR04.pdf> . [Accessed: 21-Nov-2022].

[9] "Control volumes - continuity equation," S.B.A. Invent, 16-Oct-2019. [Online]. Available: <https://sbainvent.com/fluid-mechanics/control-volumes-continuity-equation/> . [Accessed: 21-Nov-2022].

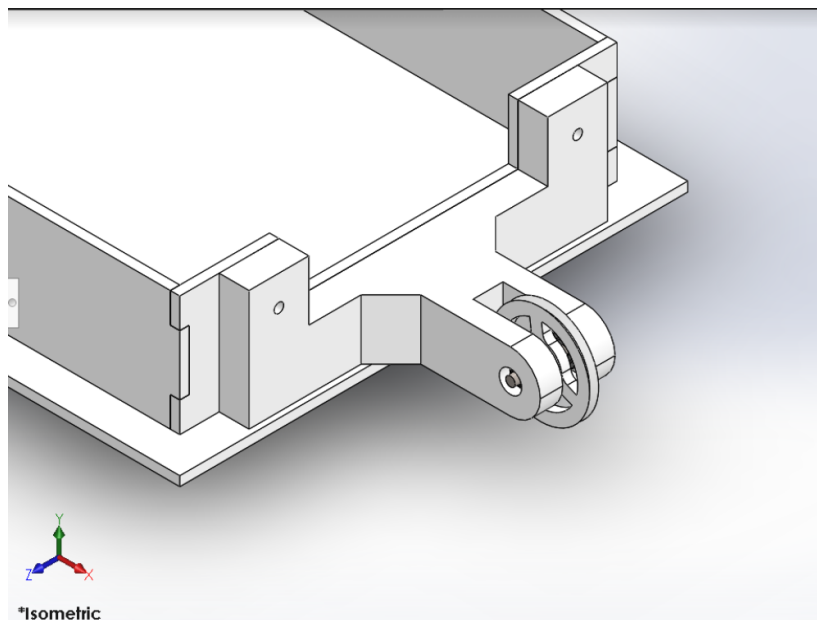
## Appendix A

<https://youtu.be/Y5LB88Cn8gE>

Appendix A1: Video sample of test with dish soap

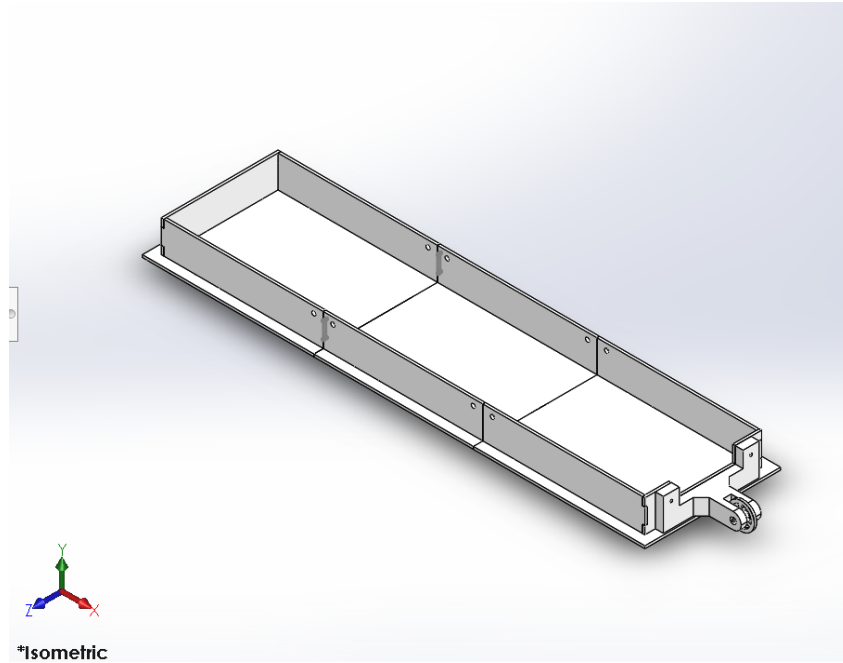


Appendix A2: Circuit diagram for ultrasonic sensor



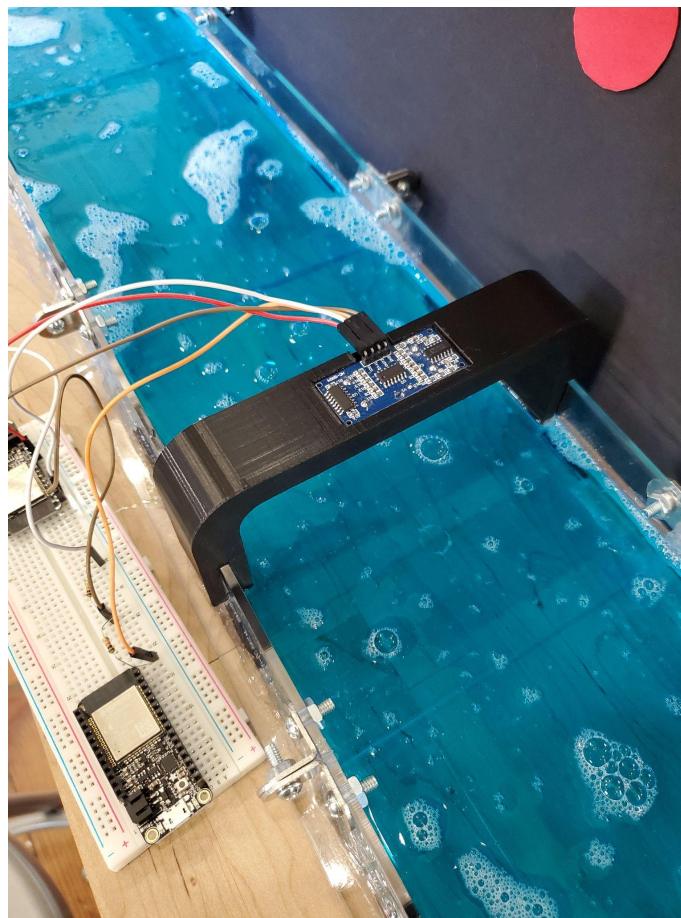
Appendix A3: Isometric view of wheel





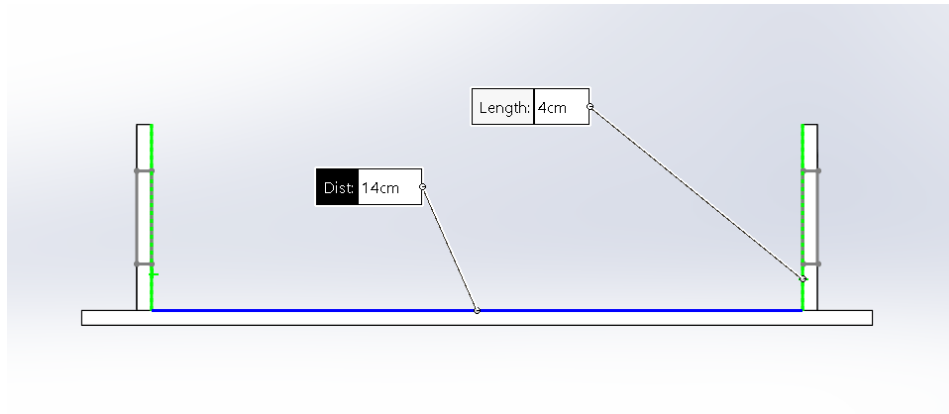
\*Isometric

Appendix A4: Isometric view of fully assembled channel

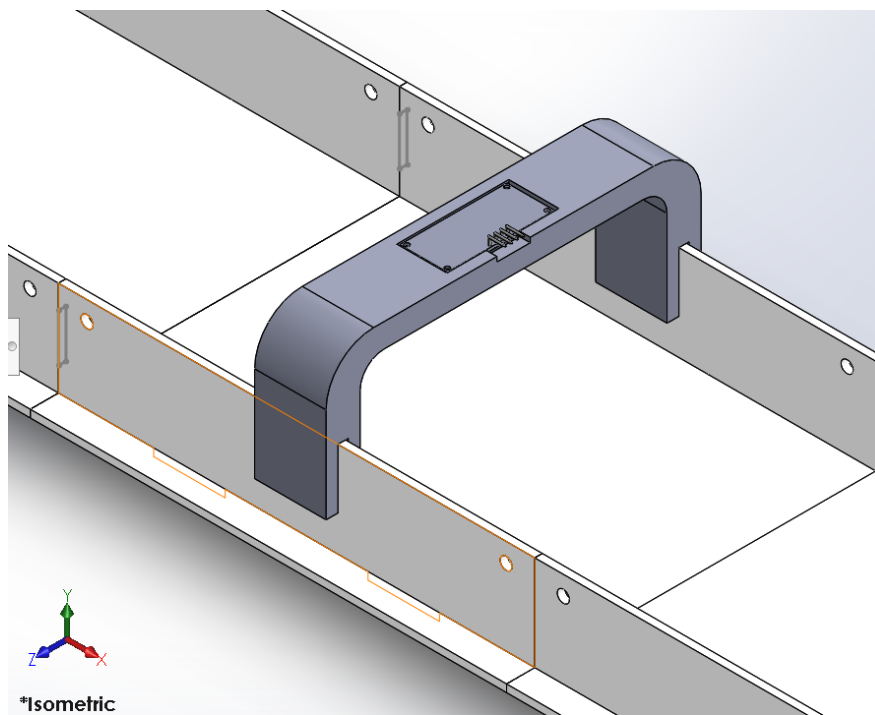


Appendix A5: Image of the wired ultrasonic sensor on the bridge



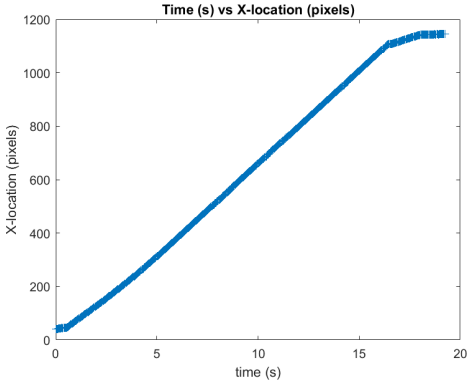
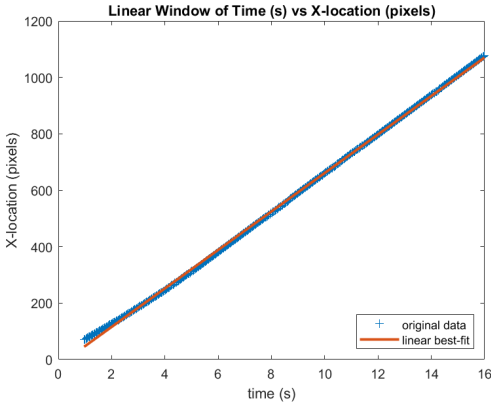
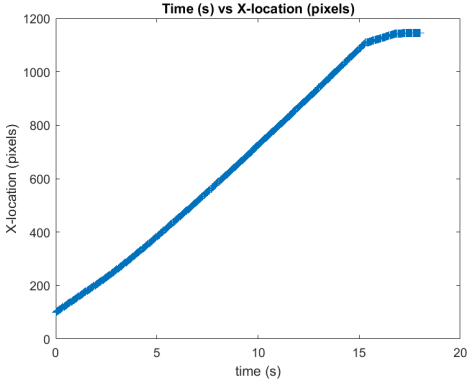
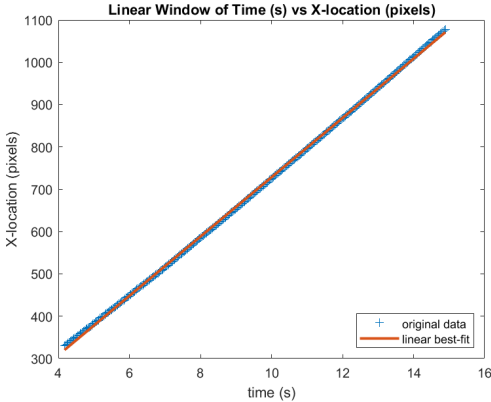
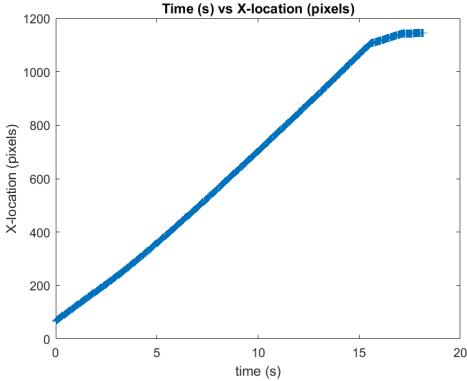
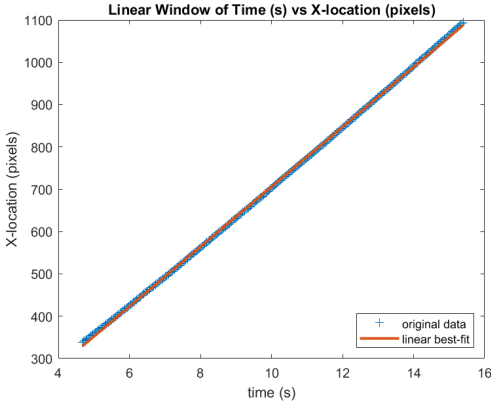


Appendix A6: Cross sectional view of the channel and its dimensions

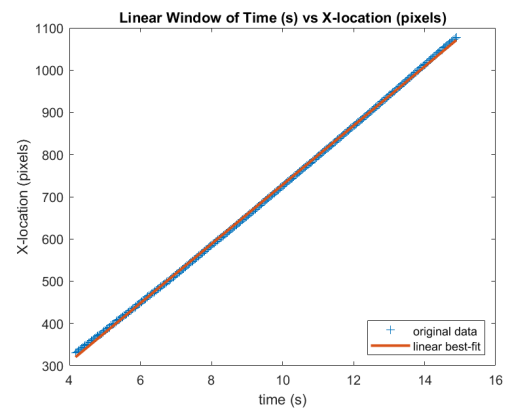
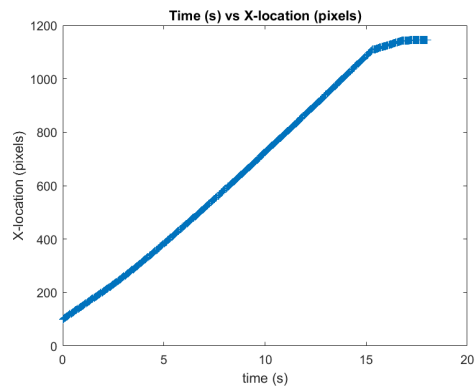


Appendix A7: Isometric view of the bridge placed on the channel

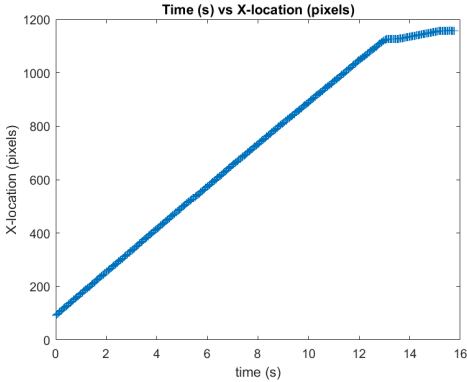
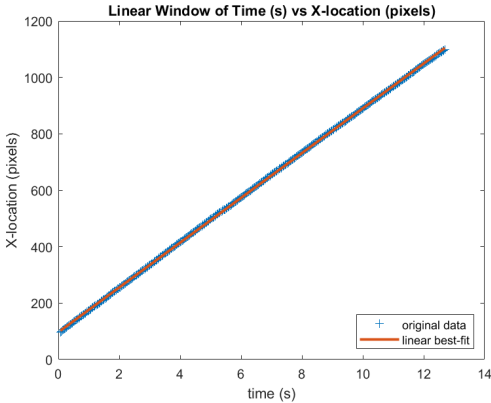
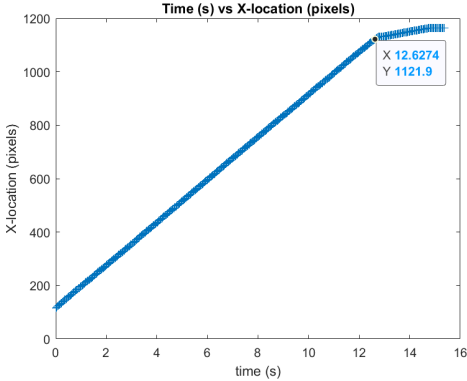
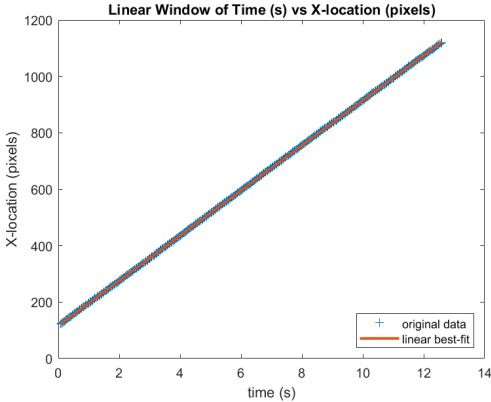
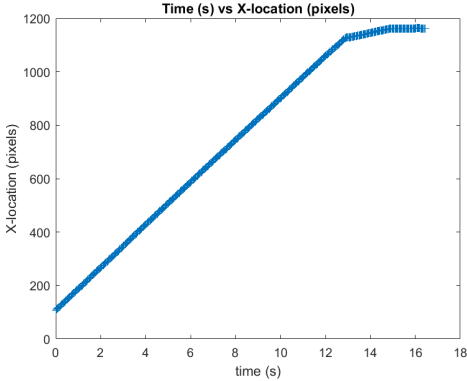
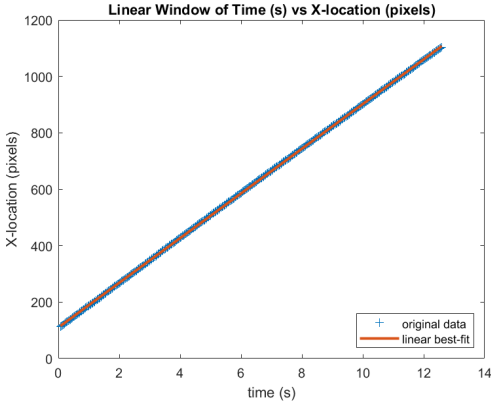
**Table A8: Raw location tracking data and windowed + linearly fitted data for dish soap trials at depth 0.662 cm**

Trial	Raw Data	Linear Window and Fit
1		
2		
3		

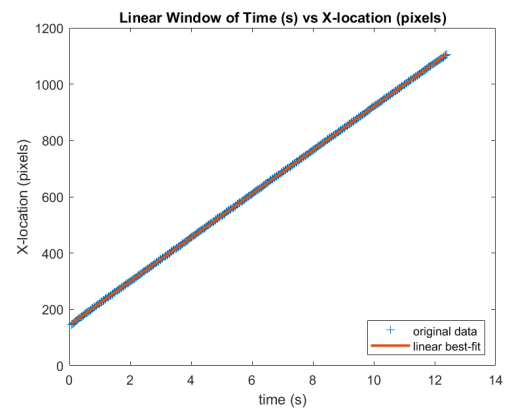
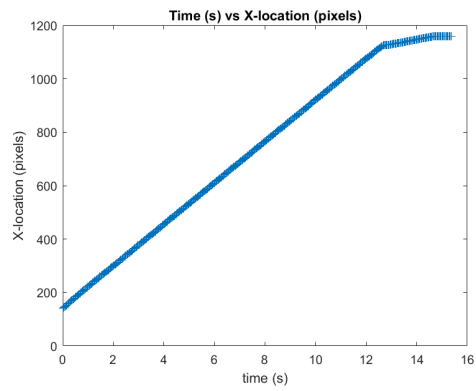
4



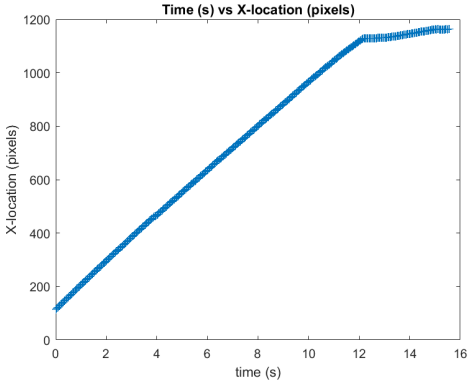
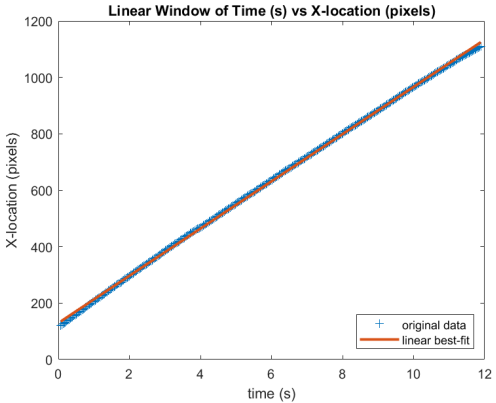
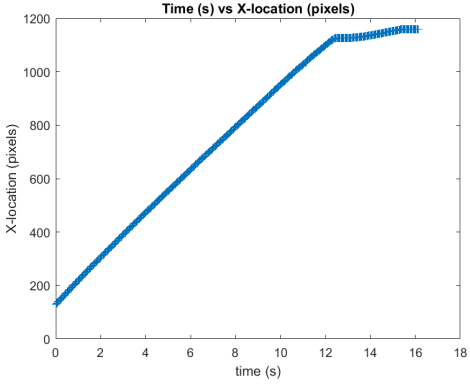
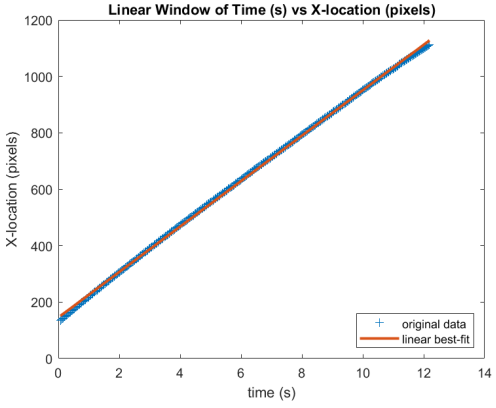
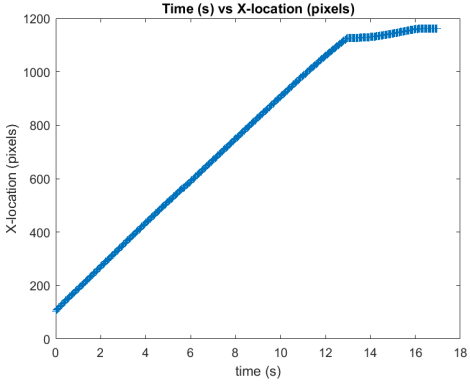
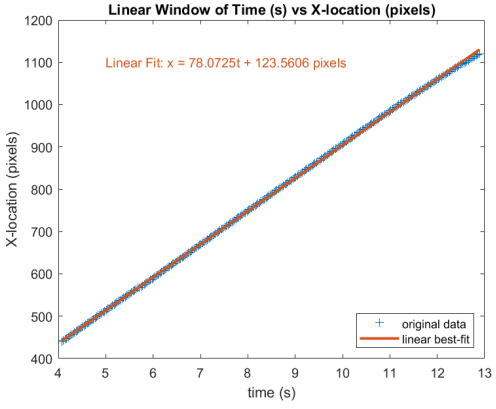
**Table A9: Raw location tracking data and windowed + linearly fitted data for dish soap trials at depth 1.062 cm**

Trial	Raw Data	Linear Window and Fit
1		
2		
3		

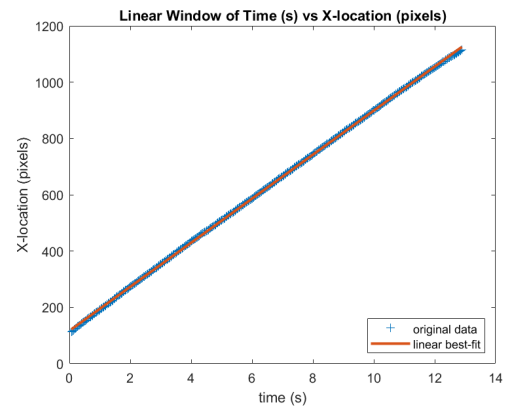
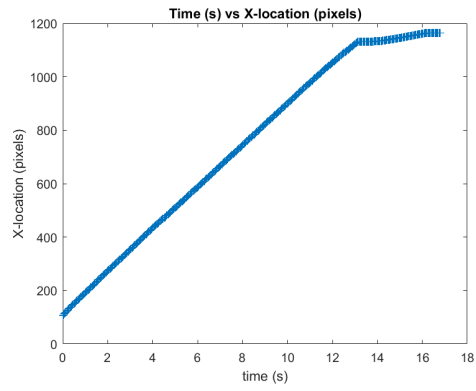
4



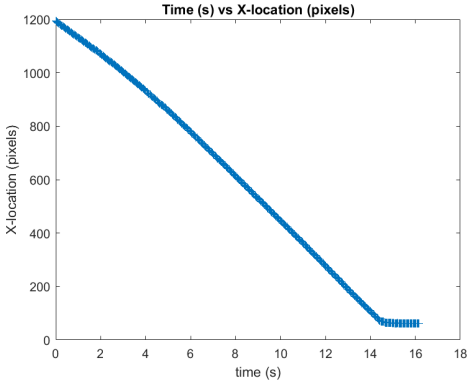
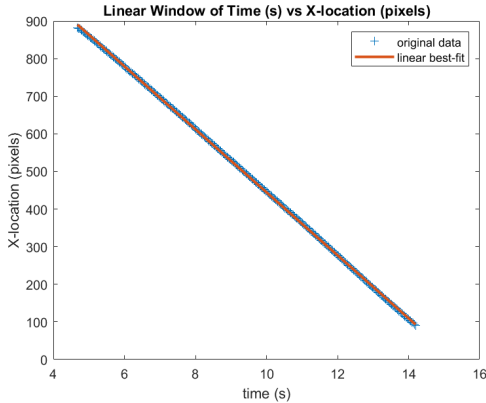
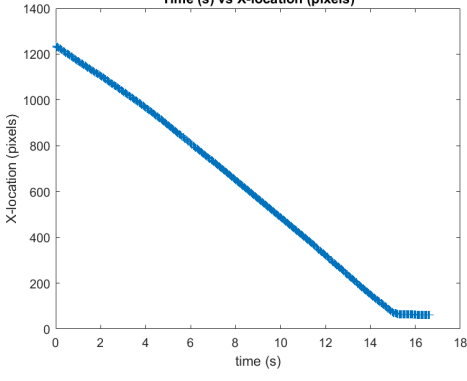
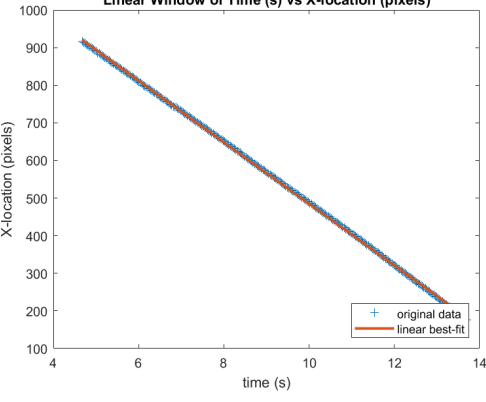
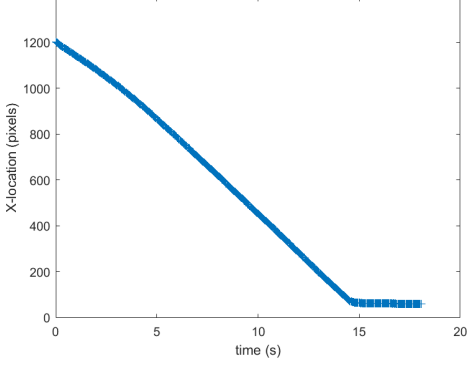
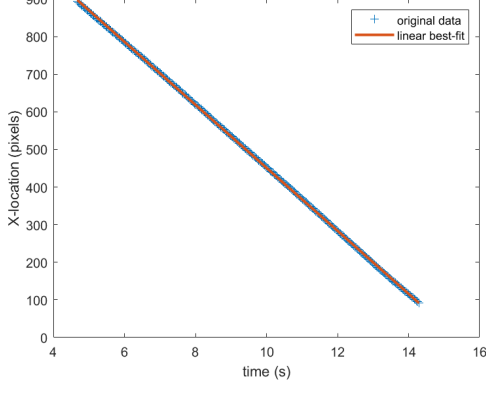
**Table A10: Raw location tracking data and windowed + linearly fitted data for dish soap trials at depth 1.452 cm**

Trial	Raw Data	Linear Window and Fit
1		
2		
3		

4



**Table A11: Raw location tracking data and windowed + linearly fitted data for corn syrup trials at depth 0.86 cm**

Trial	Raw Data	Linear Window and Fit
1		
2		
3		



4

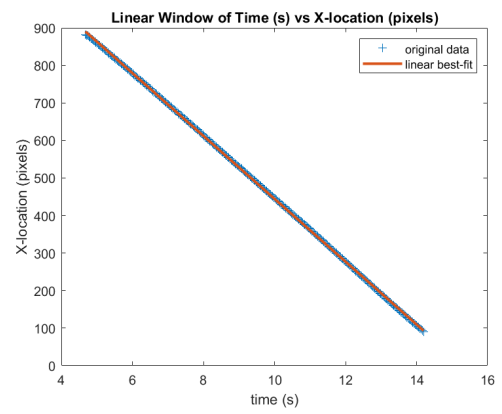
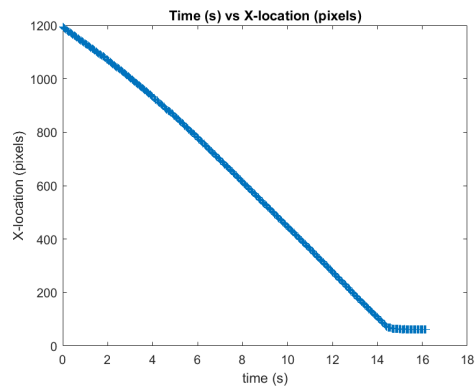
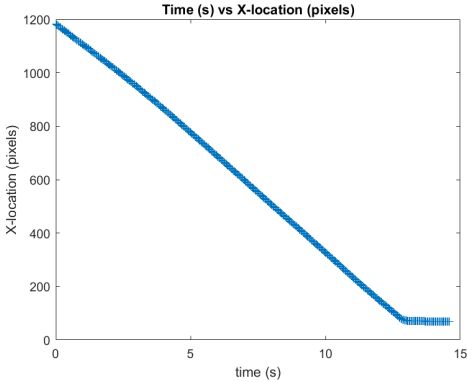
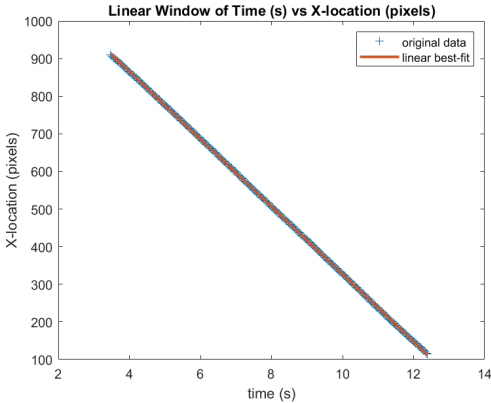
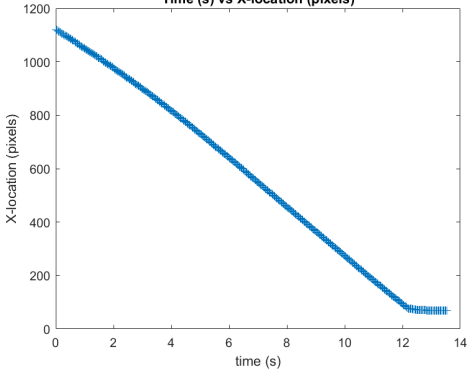
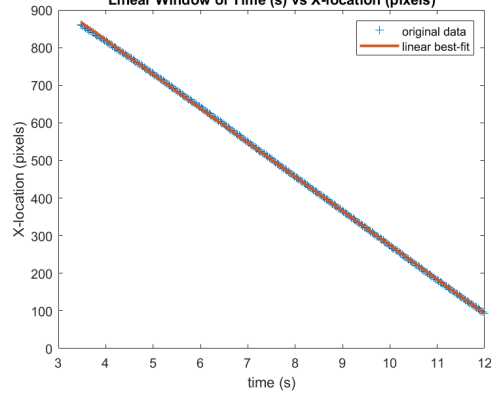
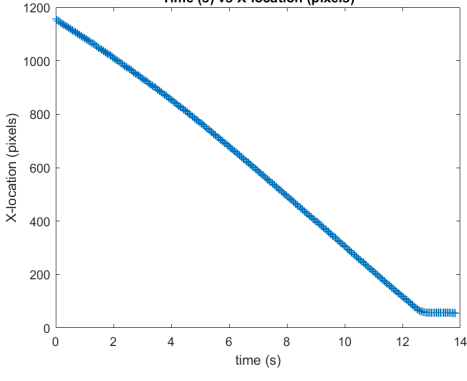
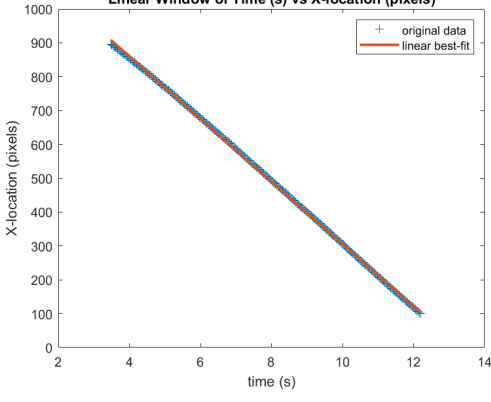
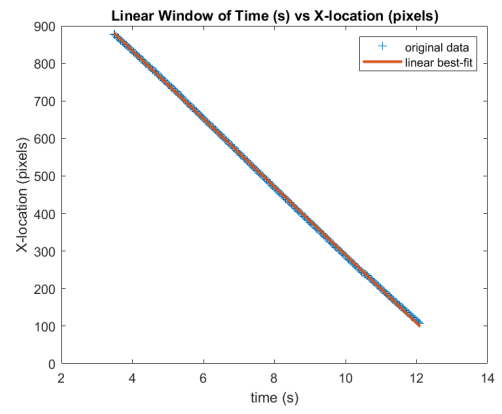
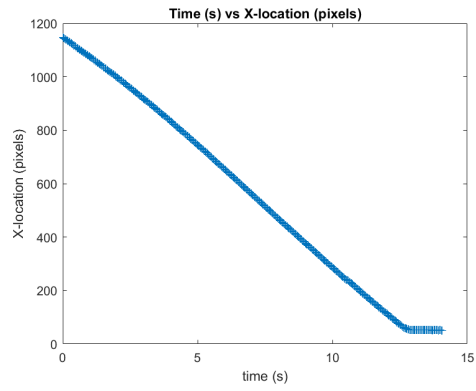


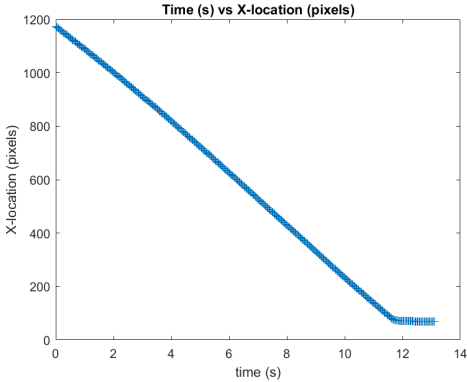
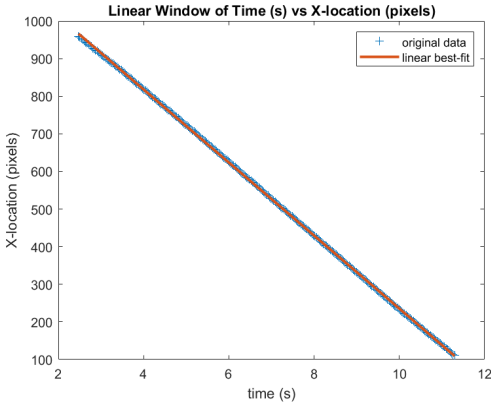
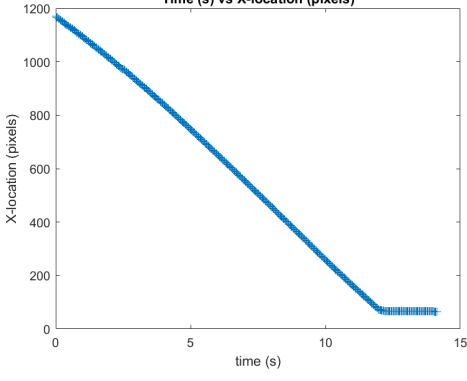
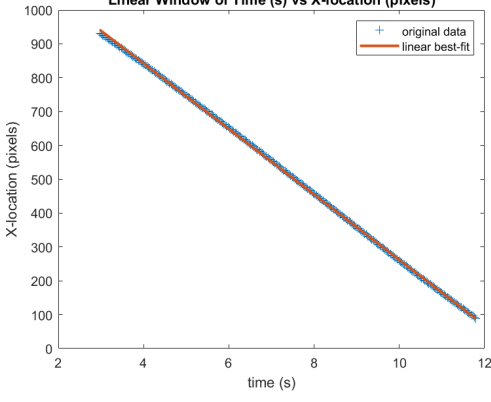
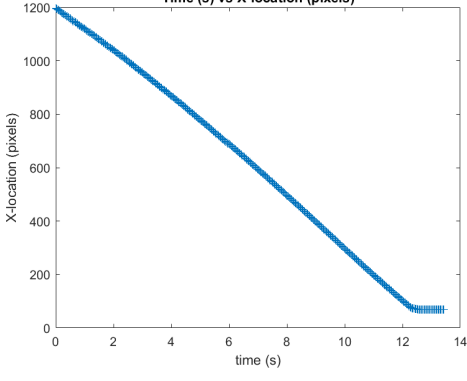
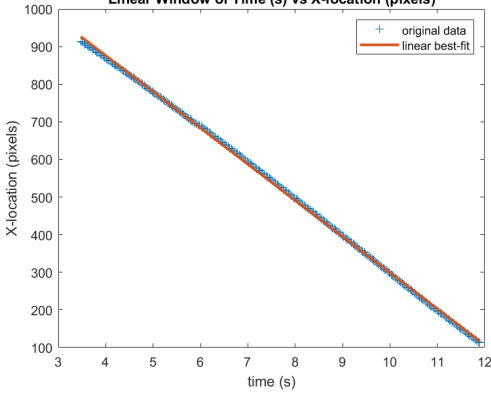
Table A12: Raw location tracking data and windowed + linearly fitted data for corn syrup trials at depth 1.056 cm

Trial	Raw Data	Linear Window and Fit
1		
2		
3		

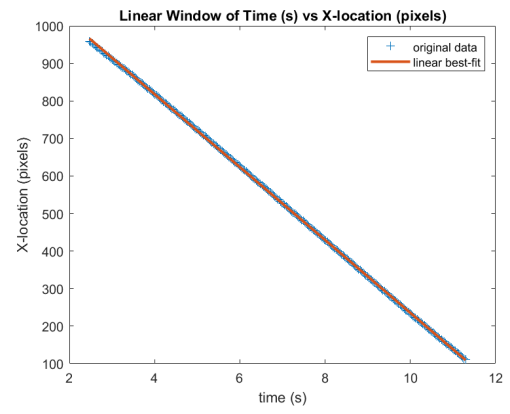
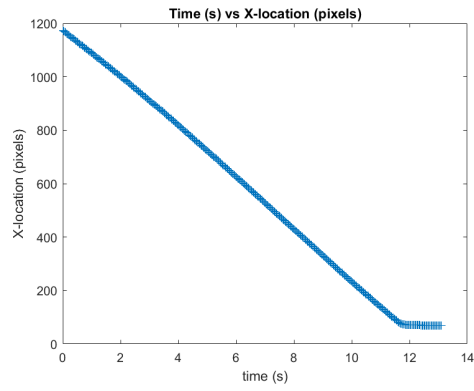
4



**Table A13: Raw location tracking data and windowed + linearly fitted data for corn syrup trials at depth 1.288 cm**

Trial	Raw Data	Linear Window and Fit
1		
2		
3		

4



## Appendix B

### Theoretical viscosity calculator as a function of inputs

```
% variables to change
full_depths = [4.34, 4.34, 4.34, 4.34, 4.4]; % array of values in cm
speed = 7.5812; % cm/s
force = 51; % g

% constants
Area = 0.09495 * 0.08555; %m^2 18
empty_depth = 5.64; % array of values in cm

% conversions
true_depths = (full_depths - empty_depth) *-1;
avg_depth = mean(true_depths) / 100;
newton_force = force/1000 * 9.8;
converted_speed = speed / 100;

% VISCOSITY
v = newton_force * avg_depth / Area / converted_speed;
result = ['dynamic viscosity = ', num2str(v), ' Pa * s']
```

result =

'dynamic viscosity = 10.4534 Pa \* s'

#### Appendix B1: Viscosity Calculator Script

## Contents

- Read Data
- Boat Tracking Imaging parameters (FOR TESTING ONLY)
- Red Encoder Circle Imaging
- Optimizing edging (FOR TESTING ONLY)
- Tracking boat (\* MAIN SECTION \*)
- DATA PROCESSING PART 1
- DATA PROCESSING PART 2 (requires manual parameter changing)
- Key Outputs
- Function for tracking

```
clc; clear all;
```

## Read Data

```
Corn = VideoReader('Corn 1.mp4');
```

## Boat Tracking Imaging parameters (FOR TESTING ONLY)

```
frame = read(Soap,1); green = frame(:,:,2); blur = imgaussfilt(green, 4); final = imbinarize(blur, .7); edges = edge(final); imshow(edges)
```

## Red Encoder Circle Imaging

Takes a random frame from video and finds X-pixel distance between red encoder circles in the background

```
snap = read(Corn,Corn.NumFrames);
redchannelcircles = snap(:,:,1);
blurred = imgaussfilt(redchannelcircles, 4);
finalred = imbinarize(blurred, .7);
edgesred = edge(finalred);
imshow(edgesred);
centersred = imfindcircles(edgesred,[12 24]);
x_red = centersred(:,1);
Matrix = sort(x_red);

% calculate the number of pixels per 10 cm distance through averaging
spacing = diff(Matrix);
spacing_filtered = spacing(2:end);
Avg = mean(spacing_filtered);
pixels_per_cm = Avg/10;           % PIXELS PER CENTIMETER
```

### Optimizing edging (FOR TESTING ONLY)

```
green_Channel = snap(:,:,2); % green channel blurr_Channel = imgaussfilt(green_Channel, 4); final_image = imbinarize(blurr_Channel, .79); edge_image = edge(final_image); imshow(edge_image);
```

### Tracking boat (\* MAIN SECTION \*)

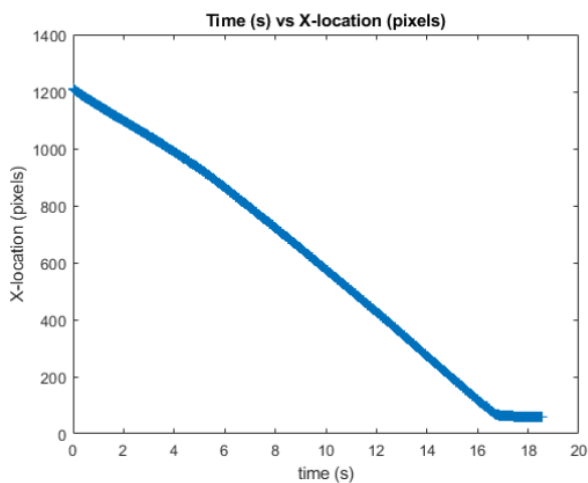
finds x-pixel position of boat at every frame (see track\_ball function)

```
pixel_pos = track_ball(Corn);
```

### DATA PROCESSING PART 1

Plotting raw data

```
time = linspace(0, Corn.NumFrames/Corn.FrameRate, Corn.NumFrames);  
time = time';  
plot(time, pixel_pos, "+");  
title("Time (s) vs X-location (pixels)");  
xlabel("time (s)");  
ylabel("X-location (pixels)");
```



### DATA PROCESSING PART 2 (requires manual parameter changing)

Linear Window by inspection

```
left_lim = 5; % CHANGE (seconds)  
right_lim = 10; % CHANGE (seconds)  
time_limited = time(left_lim * Corn.FrameRate : right_lim * Corn.FrameRate);  
pixel_pos_limited = pixel_pos(left_lim * Corn.FrameRate : right_lim * Corn.FrameRate);  
plot(time_limited, pixel_pos_limited, "+");  
title("Linear Window of Time (s) vs X-location (pixels)");  
xlabel("time (s)");  
ylabel("X-location (pixels)");  
hold on;  
  
% Line of best fit on truncated data  
fit_obj = fit(time_limited, pixel_pos_limited, 'poly1');  
velocity = fit_obj.p1 / pixels_per_cm  
ci = confint(fit_obj);  
velocity_uncertainty = (ci(2) - ci(1)) / (2 * pixels_per_cm)  
plot(time_limited, fit_obj.p1 * time_limited + fit_obj.p2, 'LineWidth', 2);  
legend("original data", "linear best-fit", 'Location', 'northeast');
```



## Key Outputs

```
A = [pixels_per_cm, " pixels per cm"]  
B = [velocity, "cm per second"]
```

A =

1×2 string array

"12.6691"    " pixels per cm"

B =

1×2 string array

"-5.5487"    "cm per second"

## Function for tracking

```
function pixel_pos = track_ball(vid)  
    pixel_pos = zeros(vid.NumFrames,1);  
    for frameNo = 1:vid.NumFrames  
        frame = read(vid,frameNo);  
        green = frame(:, :, 2);  
        blur = imgaussfilt(green, 4);  
        final = imbinarize(blur, .7);  
        edges = edge(final);  
        centers = imfindcircles(edges,[12 24]);  
        x_position = centers(1);  
        pixel_pos(frameNo) = x_position;  
    end  
end
```

## TREND ANALYSIS

```
% Constants
Area = 0.09495 * 0.08555;

% To-Change
force = 51; % g
newton_force = force/1000 * 9.8;
theoretical_viscosity = 2000; % cP
avg_meas_vel = [6.343875, 7.156225, 7.642166667]; % cm/s
avg_meas_visc = [8356.625, 9079.825, 10370.7]; % cP
depths = [0.86, 1.056, 1.288]; % cm

% Viscosity Trend analysis
plot(depths, avg_meas_visc, 'o');
hold on;
yline(theoretical_viscosity);
xlabel('Depth (cm)');
ylabel('Viscosity (cP)');
title('Measured & Theoretical Viscosities vs Depth (Karo)');
P = polyfit(depths, avg_meas_visc, 1);
plot(depths, P(1) * depths + P(2), 'r--');
legend('Measured Viscosities', 'Theoretical Viscosity', 'Linear Fit', 'Location', 'northwest');
text(depths(1), P(1) * depths(1) + 0.7 * P(2), ['d\mu/dy = ' num2str(P(1)) ' cP / cm'], 'Color', 'red');
text(depths(1), P(1) * depths(1) + 0.8 * P(2), ['linear fit : \mu = ' num2str(P(1)) 'y + ' num2str(P(2))], 'Color', 'red');

% Velocity Profile trend analysis
theoretical_velocities = newton_force / (Area * theoretical_viscosity / 1000) * depths;
figure; hold on;
plot([0 depths], [0 theoretical_velocities]);
plot([0 depths(1)], [0 avg_meas_vel(1)], '-x');
plot([0 depths(2)], [0 avg_meas_vel(2)], '-x');
plot([0 depths(3)], [0 avg_meas_vel(3)], '-x');

% Fit 2nd order polynomial to the velocity measured as a function of depth
P = polyfit([0 depths], [0 avg_meas_vel], 2);

f1 = polyval(P, [0 depths]);
plot([0, depths], f1, 'r--');
title('Velocity vs Depth at Constant Fluid Viscosity (Karo)');
xlabel('Velocity (cm/s)');
ylabel('Depth (cm)');
legend('Theoretical Linear Velocity Gradient', 'Shallow Linear Velocity Gradient', 'Medium Linear Velocity Gradient', 'Deep Linear Velocity Gradient', '2nd Order Polyfit', 'Location', 'northwest');
text(depths(1)*0.5, avg_meas_vel(1) * 1.5, ['Polyfit: U = ' num2str(P(1)) 'y^2 + ' num2str(P(2)) 'y + ' num2str(P(3))], 'Color', 'red');
```

## Appendix B3: Trend Analysis Script

## Uncertainty Calculator

```
% FIXED Uncertainties
u_mass = 0.0001 / 2; % +/- kg
u_caliper = 0.00001 / 2; % +/- m
u_F = u_mass * 9.8;
u_A = sqrt(u_caliper^2 * 0.09495^2 + u_caliper^2 * 0.08555^2);

% VARIABLE Uncertainties
u_velocities = [0.0125 0.0072 0.0057 0.0058] ./ 100; % TODO +/- m/s
u_depth = 0.003 / 2; % +/- m

% FIXED measurements
A = 0.09495 * 0.08555; %m^2

% VARIABLE measurements
mass = 51; % g TODO
depths = 0.86 * ones(1, 4); % cm TODO
velocities = [5.8877 6.4246 6.5265 6.5367]; % cm/s TODO

% Conversion calculations
F = mass / 1000 * 9.8;
y = depths ./ 100;
U = velocities ./ 100;

% Average measurement and uncertainty calculations
U_avg = mean(U);
y_avg = mean(y);
u_avg_vel = sqrt(sum(u_velocities.^2)) / 4;

u_avg_depth = u_depth / sqrt(4);
```

```

% Partial derivatives evaluated individual trials
dmudF = y ./ (A*U);
dmudy = F ./ (A*U);
dmudA = - (F*y) ./ (A^2 * U);
dmudU = - (F*y) ./ (A * U.^2);

% Uncertainty Calcs Individual
u_viscosities = [0 0 0 0];
for i = 1:4
    t1 = dmudF(i)^2 * u_F^2;
    t2 = dmudy(i)^2 * u_depth^2;
    t3 = dmudA(i)^2 * u_A^2;
    t4 = dmudU(i)^2 * u_velocities(i)^2;
    u_viscosities(i) = sqrt(t1 + t2 + t3 + t4);
end

% partial derivatives evaluated at averages
DmuDF = y_avg / (A*U_avg);
DmuDy = F / (A*U_avg);
DmuDA = - (F*y_avg) / (A^2 * U_avg);
DmuDU = - (F*y_avg) / (A * U_avg^2);

% Uncertainty of average viscosity
T1 = DmuDF^2 * u_F^2;
T2 = DmuDy^2 * u_avg_depth^2;
T3 = DmuDA^2 * u_A^2;
T4 = DmuDU^2 * u_avg_vel^2;
u_visc_avg = sqrt(T1 + T2 + T3 + T4);

u_visc_cP = u_viscosities * 1000
u_visc_avg_cP = u_visc_avg * 1000
u_avg_vel_cms = u_avg_vel * 100

```

Appendix B4: Uncertainty Calculator Script